

The Surfacing of Multiview 3D Drawings via Lofting and Occlusion Reasoning

Enhanced version improved over camera-ready

Anil Usumezbas
SRI International

201 Washington Rd, Princeton, NJ 08540, USA

anil.usumezbas@sri.com

Ricardo Fabbri

Polytechnic Institute – Rio de Janeiro State University

R. Bonfim 25, Vila Amelia, Nova Friburgo RJ 28625-570, Brazil

rfabbri@gmail.com

Benjamin B. Kimia

Brown University

Providence, RI 02912, USA

benjamin.kimia@brown.edu

Abstract

The three-dimensional reconstruction of scenes from multiple views has made impressive strides in recent years, chiefly by methods correlating isolated feature points, intensities, or curvilinear structure. In the general setting, i.e., without requiring controlled acquisition, limited number of objects, abundant patterns on objects, or object curves to follow particular models, the majority of these methods produce unorganized point clouds, meshes, or voxel representations of the reconstructed scene, with some exceptions producing 3D drawings as networks of curves. Many applications, e.g., robotics, urban planning, industrial design, and hard surface modeling, however, require structured representations which make explicit 3D curves, surfaces, and their spatial relationships. Reconstructing surface representations can now be constrained by the 3D drawing acting like a scaffold to hang on the computed representations, leading to increased robustness and quality of reconstruction. This paper presents one way of completing such 3D drawings with surface reconstructions, by exploring occlusion reasoning through lofting algorithms.

1. Introduction

Dense 3D surface reconstruction is an important problem in computer vision which remains challenging in general scenarios. Most existing multiview reconstruction methods suffer from some common problems such as: (i) Holes in the 3D model corresponding to homogeneous/reflective/transparent image regions, (ii) Over-smoothing of semantically-important details such as ridges, (iii) Lack of semantically meaningful surface features, or-

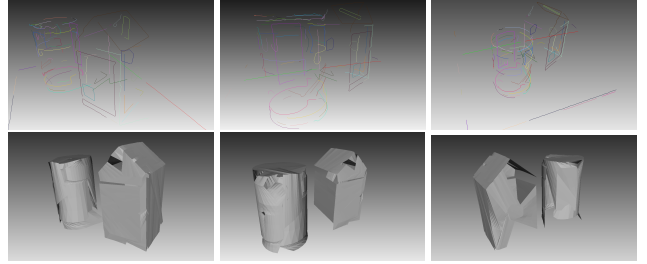


Figure 1: The proposed approach transforms a 3D curve drawing (top) obtained from a fully calibrated set of 27 views, into a collection of dense surface patches (bottom) obtained via lofting and occlusion reasoning.

ganization and geometric detail.

In computer vision and graphics literature, there has been scattered but persistent interest in using 3D curves to infer aspects of an underlying shape [28, 56], shape-related features linked to shading [6], or closed 3D curves [55]. For example, the approach in Sadri and Singh [44] exploits the *flow complex*, a structure that captures both the topology and the geometry of a set of 3D curves, to construct an intersection-free triangulated 3D shape. Similarly, the approach in Pan *et al.* [39] explores a similar concept with *flow lines*, which are designed to encapsulate principal curvature lines on a surface. As another example, the approach in Abbasnejad *et al.* [1] identifies potential surface patches delineated by a 3D curve network, breaking them into smaller, planar patches to represent a complex surface. These methods are completely automated and yield impressive results on a wide range of objects. However, they require a complete and accurate input curve network, which is very difficult to obtain in a bottom-up fashion from image data: there will always be holes, missed curves, incorrect groupings, noise, outliers, and other real-world imperfections. Fur-

thermore, these methods are not general, but rather tailored for scenes with objects of relatively clean geometry. Thus, they are not suitable for more general, large-scale complex scenes that the multiview stereo community tackles on a regular basis.

We propose a novel and complementary dense 3D reconstruction approach based on occlusion reasoning and a CAD method called *lofting*, which is the process of obtaining 3D surfaces through the interpolation of 3D structure curves. Lofting has primarily been a drafting technique for generating streamlined objects from curved line drawings that was initially used to design and build ships and aircrafts. More recently, lofting has become a common technique in computer graphics and computer-aided design (CAD) applications where a collection of surface curves are used to define the surface through interpolation. Even though lofting is a very powerful tool, it does not appear to be used very much in the multiview geometry applications. Employing an existing curve-based reconstruction method, we start with a calibrated image sequence to build a 3D drawing of the scene in the form of a 3D graph, where graph links contain curve geometries and graph nodes contain junctions where curve endpoints meet. We propose to use the 3D drawing of a scene as a scaffold on which dense surface patches can be placed on, see Figure 1. Our approach relies on the availability of a “3D drawing” of the surface, a graph of 3D curve fragments reconstructed from calibrated multiview observations of an object [51]. Observe that such a 3D drawing acts as a scaffold for the surface of the object in that the drawing breaks the object surfaces into 3D surface patches, which are glued on and supported by the 3D drawing scaffold. Our approach then is based on selecting some 3D curve fragments from the 3D drawing, forming surface hypotheses from these curve fragments, and using occlusion reasoning to discard inconsistent hypotheses.

Aside from yielding a useful and semantically-meaningful intermediate representation, reconstructing surfaces by going through curved structures closely replicates the human act of drawing: As in a progressive drawing, the basis is independent of illumination conditions and other details. For instance, photometry/shading/reflectance can be incorporated later on either as hatchings or progressively refined as fine shading; multiple renderings can be performed from the same basis. Even challenging materials such as the ocean surface can be rendered on top of a curve basis. This approach also has the advantage of scalability, since it allows for a very large 3D scene to be selectively and progressively reconstructed.

This paper is organized as follows: Section 2 reviews the state-of-the-art in generating a 3D drawing of a scene observed under calibrated views. Section 3 reviews lofting and describes how a surface is generated from a few curve fragments lying on the surface. Section 4 describes

how 3D surface patch hypotheses are generated from a 3D drawing, and how occlusion consistency is used to take out non-veridical hypotheses. Section 6 deals with several technical challenges, which require a regularization of the 3D drawing so that surface patches can be robustly inferred. Section 6 presents experimental results, a comparison with PMVS [12, 13], and quantification of reconstruction accuracy.

2. From Image Curves to a 3D Curve Drawing

Our multiview stereo method is based on the idea of using 3D curvilinear structures as boundary conditions to hypothesize the simplest 3D surfaces that would be explained by these boundaries. The 3D curvilinear structure that is needed is obtained by correlating image curves in calibrated multiview imagery to reconstruct 3D curve fragments, which are organized as a graph and referred to as “3D Curve Drawing” [51]. Since this paper requires a 3D curve drawing available, we summarize the work of [51] on which we rely.

The 3D curve drawing is built on a series of steps. First, the image is pre-processed to obtain edges using robust, third-order operators which give highly-accurate edge information [49]. Second, a geometric linker groups edges into curves [18] which claims to improve on grouping errors and extent of outliers. This results in image curve fragments $\gamma_i^v, i = 1, \dots, M^v$ for each view $v = 1, \dots, N$. Third, pairs of curves $(\gamma_{i_1}^{v_1}, \gamma_{i_2}^{v_2})$ from two “hypothesis views” v_1 and v_2 , which have significant epipolar overlap, are used to generate putative candidate reconstructions $\Gamma_k, k = 1, \dots, K$. These candidate reconstructed curves are gauged against image evidence on other projected views called “confirmation views” and if there is sufficient support for a 3D curve candidate, it is confirmed and otherwise rejected. This results in a set of unorganized 3D curve fragments called the “3D Curve Sketch”.

This representation indeed resembles a sketch. 3D curve fragments in this sketch are often redundant since they came from multiple hypotheses, are often overfragmented due to partial epipolar overlap, feature a nontrivial level of clutter, and most importantly, are unorganized in that the topological relationship of 3D curve fragments is not available. The recent work of [51] deals with these issues, and constructs a graph of 3D curve fragments referred to as a 3D drawing of the scene.

Our approach requires 3D curve fragments and their topological relationships. To the best of our knowledge, the approach in [51] is the state of the art in curve-based multiview stereo. However, any other method that can give 3D curve fragments organized in a topological graph can be used by our approach as well.

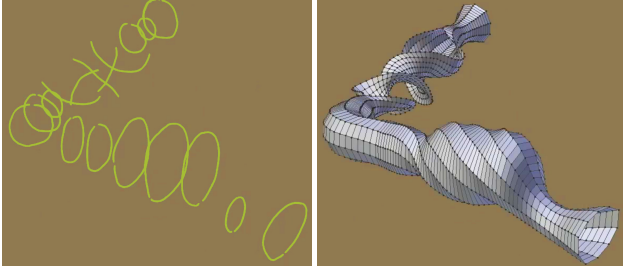


Figure 2: From open and closed curves (left), lofting produces smooth surfaces (right).

3. Bringing Lofting Into Multiview Stereo

Lofting is graphics technique for shape inference from a set of 3D curves, a term with roots in shipbuilding to describe the molding of a hull from curves [5]. Designers often use such intermediate, curve-based representations (sketches, graphs, drawings) to outline 3D shape, as they compactly capture rich 3D information and are easy to customize. Through lofting, these 3D curves are used to interactively model smooth surfaces, Figure 2. Implementations of lofting are commonplace in interactive CAD [3, 54, 38, 30, 17, 1, 9, 31], and applications [25, 2, 50]. Lofting has not yet spread to 3D computer vision, where fully-automated image-based modeling is the norm. This work leverages lofting to build a fully-automated, dense multiview stereo reconstruction pipeline.

Given 3D curves $\Gamma_1, \Gamma_2, \dots, \Gamma_n$ forming the partial boundary of a surface, lofting produces a smooth surface passing through them which is sought to be ‘simple’: smooth, avoiding holes and degeneracies such as self-intersections. Earlier approaches formulated this as surface deformation with parameters estimated to fit the prior into a 3D curve outline [8, 21]. Approaches using functional optimization [30, 38, 46, 52, 4, 29] employ generic objectives, such as least squares and integral of squared principal curvatures, and the result depends on this choice, leading to overfitting or oversmoothing. These approaches cannot easily handle complex shapes with many self occlusions [25]. Other algorithms include those based on B-splines [53, 41].

We have chosen lofting based on subdivision surfaces, a well-known graphics technique that divides the faces of a coarse input mesh via a recursive sequence of transforms or subdivision schemes, yielding smooth high-poly meshes, Fig. 3. Subdivision is widely used in a number of graphics problems [42, 10], such as surface fitting [47, 48, 27], reconstruction [19, 28, 56], and lofting itself [32, 34, 35, 37, 36, 7]. Combined subdivision schemes [24, 23] translate conditions on the limit surface to conditions on the scheme itself, and allow subdivision to be adjusted near the curve network and boundary conditions beyond subdivision or spline curves. Subdivision surfaces provide a simple standard framework, with more powerful schemes compared to other techniques; meshes with

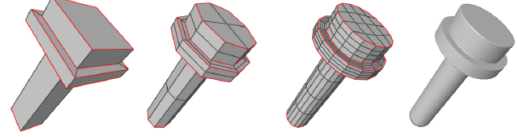


Figure 3: Application of subdivision resulting in a high-poly surface (manually marked hard edges in red) [22].

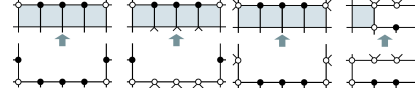


Figure 4: Quadtrangulation in lofting; depending on the configuration of special interior vertices on a chain, one of these edits are applied to obtain a base mesh topology [45].

complex constraints at corners can be handled with greater ease [45]. We leverage [45], which takes open 3D polygonal lines terminating in a set of corners – as in our 3D drawing, but interactively generated. We have augmented it to automatically reorganize the curve network prior to lofting, and with additional heuristics to avoid degeneracies. The result is a lofting approach that can: i) take any number of boundary curves partially or completely covering the boundary of the desired surface, and ii) handles topological inconsistencies, self-intersections, discontinuities and other geometric artifacts. A brief description of our lofting stage follows.

Skinning: quadtrangulates the input curves to construct a quad topology base mesh without the final geometry [45, 43, 20, 33]. Skinning does not produce accurate shape approximation, but mainly avoids vertices lacking curvature continuity [26]. Given a closed 3D curve $\Gamma = (s_1, \dots, s_n)$, a chain is a subsequence $\Gamma_{i+k}^{i+k} = (s_i, \dots, s_{i+k})$, $i = 1, \dots, n+k$. The topology of the base mesh λ is constructed by a sequence of chain advances on Γ : given Γ_{i+k}^{i+k} , this adds a layer of k quads to λ bounded below by Γ_{i+k}^{i+k} and above by a new chain $\bar{\Gamma}_{j+k}^{j+k} = (s_j, \dots, s_{j+k})$ on the interior of the resulting patch λ . Γ is replaced by $\tilde{\Gamma} = \Gamma_1^{i-1} \cup \bar{\Gamma}_j^k \cup \Gamma_{i+k+1}^n$. Depending on the configuration of special interior vertices, different types of advances apply [45], Fig. 4.

Fairing computes the positions of the vertices in λ by minimizing “fairness” energy, a thin-plate functional [45]. **Subdivision** is then applied with a modified version of Catmull-Clark schemes [45], yielding a fine mesh, see Figure 3.

4. Automated Multiview Reconstruction Using Lofting

In the previous two sections, we described: (i) The concept of a *3D curve drawing*, a graph of 3D contour fragments and a method for deriving it from a set of calibrated multiview imagery, and (ii) the concept of lofting which reconstructs 3D surface meshes bounded by a set of given contour fragments. We now describe how *pairs of curve*

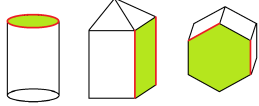


Figure 5: A schematic of a simple shapes where a surface patch (green) is represented by a pair of curves (red); in the case of closed curves, a pair is not necessary.

fragments selected from the 3D curve drawing give rise to 3D surface hypotheses. These hypotheses are then ruled out when they predict occlusions which are not consistent with the input data. The remaining hypotheses yield a set of occlusion-consistent surface patches. In the following, we first describe the process of hypothesis formation and then testing of formed hypotheses for occlusion consistency.

Forming Surface Patch Hypotheses: Ideally, any subset of curve fragments should be able to form surface hypotheses, but this is clearly intractable; even if curve fragments are long, noiseless and salient (a critical factor as we shall see in Section 5), they number in the order of 100 curves or so. Note that surface patches that arise from closed curves are a special case and these be identified and processed a priori. The remaining surface patches involve at least two curve fragments but typically more, say around 3-5. Then, pairs of curve fragments can be used as entry level hypotheses, Figure 5.

The pool of curve fragments from which pairs are selected is restricted to those with a minimal length constraint, $L > \tau_{length}$. This threshold is learned from data and is typically around a few centimeters for our data. The distance between two 3D curves is defined as the average point-to-curve distance for all the samples on both curves. The typical 3D curve proximity threshold τ_α , which is also learned from data, is around 15-20 cm.

Third, in addition to length and pair proximity, curvature of the reconstructed surface is a cue to whether it is veridical. This is because object surfaces are typically not as convoluted as surfaces arising from unrelated cues. We use average Gaussian curvature, *i.e.* Gaussian curvature at every point on the surface averaged over all surface points, and a threshold τ_G which is also learned. It should be noted that every curve pair generates two surface hypotheses: each endpoint in a given curve can pair with two possible endpoints on the other curve in the pair. The surface hypotheses with lower average Gaussian curvature is the one that is selected, if it is above τ_G , Figure 6. See Figure 7 for a collection of sample surface hypotheses obtained this way.

Note that an alternate method for forming pairs of 3D curve fragments is to use the topology of 3D curve fragments as projected onto 2D views. The topology of 2D image curves is derived from the medial axis or Delaunay Triangulation to determine the neighboring curve fragments for any given curve. The topology of projected 3D curve fragments then induces a neighborhood relationship among

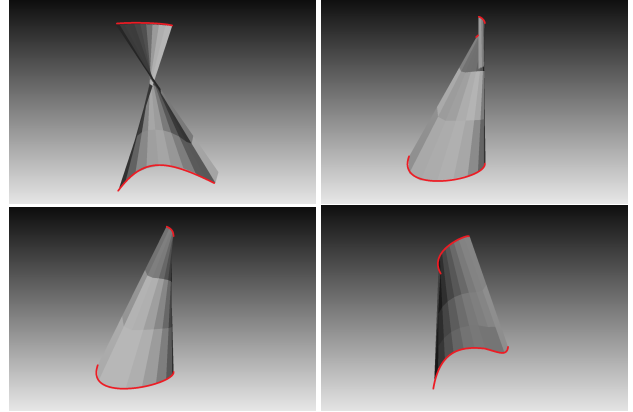


Figure 6: There is an inherent ambiguity in reconstructing a surface from two curve fragments arising from which end-points are paired (top row vs. bottom row). When two curve fragments do belong to a veridical surface, one of the two reconstructions generally has much lower average Gaussian curvature than the other and this is a cue as to which one is veridical. When the pairing of curve fragments is incorrect in that no surface exists between them, both reconstructions have high average Gaussian curvature, a cue to remove outliers.

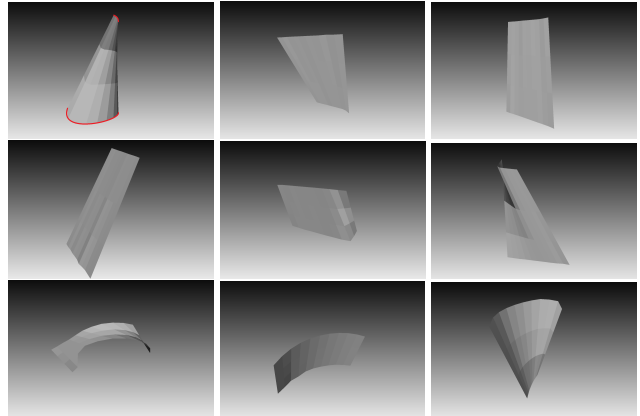


Figure 7: Some example loft surfaces of various geometries that our reconstruction algorithm generates.

3D curve fragments: two 3D curve fragments are neighbors in 3D if their corresponding 2D image curves are neighbors in at least one view. This improves the performance in two ways: (i) veridical pairing which exceed the proximity threshold are restored to the pool of candidate pairs; (ii) non-veridical curve pairs which are not neighbors are correctly discarded. This is a significant factor in areas dense in 3D curves compared to the proximity threshold, which generates numerous non-veridical curve pairs.

Hypothesis Viability Using Occlusion Consistency: The most important cue in probing the viability of a 3D surface patch hypothesis is whether it is consistent with respect to the occlusions it predicts (it is assumed that surfaces are

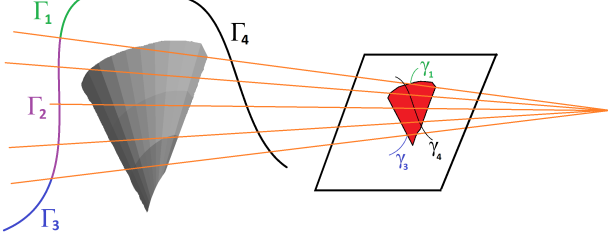


Figure 8: A 3D surface patch S occludes all 3D curve fragments that lie behind it. Thus, the 3D curve fragments between Γ_1 and Γ_4 are partially obstructed so that only portions between (Γ_1, Γ_2) and (Γ_3, Γ_4) are visible as (γ_1, γ_2) and (γ_3, γ_4) in the image. The projections of (Γ_2, Γ_3) should have no edge evidence in the image. On the other hand, the 3D curve fragments (Γ_5, Γ_6) is fully unoccluded and edge evidence for it is expected. The presence of edge evidence in the portion (γ_2, γ_3) is grounds for invalidating the 3D surface hypothesis S .

opaque). If an opaque 3D surface patch is veridical, then all 3D curve structures that are occluded by it in a given projected image must be invisible. For example, a surface hypothesis may occlude a portion of a 3D curve. Image evidence supporting the occluded portion is grounds for invalidating the surface hypothesis, Figure 8.

The technical approach to testing occlusion is based on ray tracing [16]: A ray is connected from the camera center to each point on a 3D curve fragment belonging to the 3D curve drawing and the visibility of the point is tested against each surface hypothesis. Specifically, let $\{\Pi_1, \dots, \Pi_N\}$ denote the set of hypothesized surface patches. Let the 3D curve drawing have curve fragments $\{\Gamma_1, \dots, \Gamma_K\}$, each having image curve projections onto view l , $\gamma_k^l(s)$, where s represents length parameter $s \in [0, L_k^l]$, where L_k^l is the total length of the projected curve. Let the portion of the 3D curve that is occluded by the surface patch Π_n be denoted by the interval $(a_{k,n}^l, b_{k,n}^l)$. Then, the evidence against surface hypothesis Π_n provided by curve Γ_k from view l , $E_{n,k}^l$, is the edge support for the invisible portion. This evidence is the sum of total edge support at sample point s , $\phi(\gamma_k^l(s))$, which is simply the number of image edges that have matching locations and orientations to the curve $\gamma_k^l(s)$ at sample point s :

$$E_{n,k}^l = \int_{a_{k,n}^l}^{b_{k,n}^l} \phi(\gamma_k^l(s)) ds \quad (1)$$

This evidence is then subjugated to a threshold of significance τ_E ; if significant, the evidence invalidates the hypothesis. On the other hand, if the evidence against the hypothesis for all the curves that should be occluded is indeed insignificant, *i.e.*, $E_{n,k}^l < \tau_E, \forall k$, the lack of evidence in fact provides support for the surface hypothesis. This is to be distinguished from surface hypotheses that are not oc-

cluding any curves. The situation where Π_n occludes Γ_k and image evidence shows occlusion lends more evidence to Π_n than the situation where Π_n does not occlude any curves.

We now assume that all surface patches occlude at least one curve in at least one view; note that for polyhedral shapes, frontal patches occlude the contours of patches on the back, so this is not a stringent assumption. In fact, probing this assumption on both Amsterdam House Dataset and Barcelona Pavilion Dataset (which are described in Section 6) shows that this is the case for more than 90% of the surface hypotheses generated. This assumption implies that each surface hypothesis needs to be confirmed at least once against an occlusion hypothesis, *i.e.*, $\forall n, \exists l, \exists k$, such that $E_{k,n}^l < \tau_E$.

The above process probes the implication of surface patch in relation to the 3D curve drawing. When introducing a multitude of surface patches, however, the issue of occlusion between two surface hypotheses arises. It is possible that one surface hypothesis is fully occluded by all other surfaces. Such a surface is then not visible in any view and is discarded.

Redundant Hypotheses: Since surface hypotheses are generated by pairs of 3D curve fragments, if a ground truth surface consists of multiple curve fragments, say a rectangular patch consisting of four curve fragments, then the same surface will likely be represented by a number of curve fragment pairs, six possible pairs in the case of a rectangular patch.

These redundant representations are detected in a post-processing stage and consolidated. When a large portion of a surface hypothesis (80% in our system) is subsumed by another surface, *i.e.*, 80% of the points on it are closer than a proximity threshold to another surface, then this surface is discarded as a redundant hypothesis. A more principled approach is to merge two overlapping surfaces by forming curve triplet hypotheses: When two curve pairs have a curve fragment in common and their surface hypotheses overlap, as described above, the lofting approach is applied to the curve triplet and the resulting surface replaces the pair of surface hypotheses. And, of course, a curve triplet and a curve pair with a common curve fragment and overlapping surfaces result in curve quadruplet hypotheses, and so on as needed. This growth of surface hypotheses yields more accurate and less redundant surface patches, but results from this process are not ready for inclusion in this publication.

Figure 9 is a visual illustration of our entire surface reconstruction approach. Figure 10 demonstrates that our algorithm is very good at correlating image edges with 3D curve structures, accurately reasoning about occlusion and confirming an overwhelming majority of correct surfaces, as well rejecting almost all of the incorrect hypotheses, Figure 11. It should be noted that many surface hypotheses do

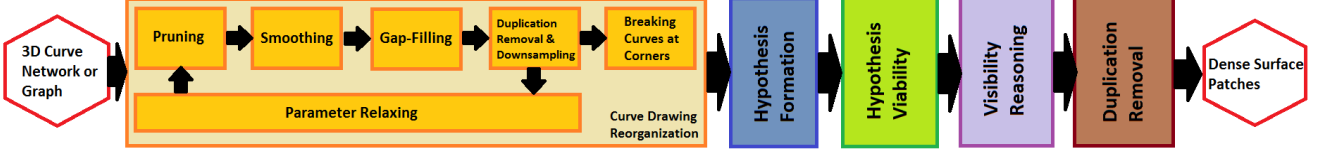


Figure 9: A visual illustration of our dense surface reconstruction pipeline.

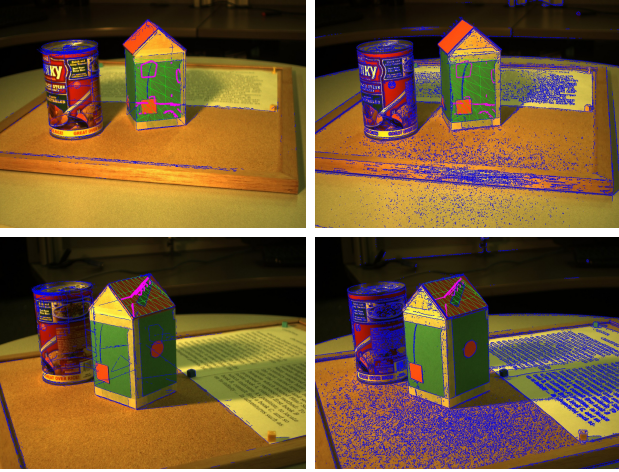


Figure 10: Examples of surface hypotheses being confirmed by the confirmation views shown here. Left column: Projected surface hypothesis is shown in green, projected curve drawing is shown in blue and occluded segments are shown in purple. Right column: Same surface and occluded segments are shown with image edges in blue. Notice the lack of any edge presence whatsoever around most of the purple segments, which is clear indication of occlusion consistency between the images and the hypothesis surface.

not contain any portion of the curve drawing behind them from *any* given view. These hypotheses cannot be confirmed or denied, and, depending on the robustness of the hypothesis generation algorithm, they can be included in or discarded from the output as needed. In addition, many existing multiview stereo methods can be plugged into our system at the level of curve pairing and used as alternative ways to provide initial seeds for our surface hypotheses. As mentioned earlier, our lofting algorithm scales well to a large number of input 3D curves, which are provided either simultaneously or sequentially.

5. Reorganization of Input Curve Graph Using Differential Geometric Cues

Four important technical issues arise in the application of lofting to reconstruct surface patches from 3D drawings.

Problem 1: Lofting sensitivity to overgrouping: Lofting is highly sensitive to overgrouping of edges into curves. If some parts of a curve belong to a veridical surface patch

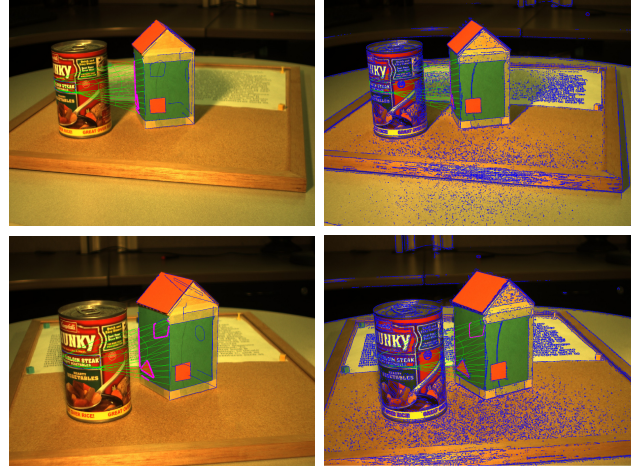


Figure 11: An example outlier surface hypothesis ruled out by detected edge structures. Left column: projected surface hypothesis is shown in green, projected curve drawing is shown in blue and occluded segments are shown in purple. Right column: Same surface and occluded segments are shown with image edges in blue. Notice how most of the purple segments are barely visible from all the edges that match in both location and orientation.

but another part does not, then the lofting results experience significant and irreversible geometric errors, *e.g.*, as in Figure 12a where two curve fragments C_1 and C_2 belong to a side of the house and correctly hypothesize a surface patch through lofting. However, if C_2 is grouped with an adjacent curve fragment C_3 belonging to an adjacent face of the house that C_2 belongs to (let C_4 denote $C_2 \cup C_3$), then the lofting results based on (C_1, C_4) do not produce a meaningful surface patch. The core of this problem is that the curve C_2 is shared by two surface hypotheses, but if grouped with C_3 , it can no longer represent the frontal surface hypothesis created by C_1 and C_2 . This transition in the ability to represent multiple surface hypotheses happens at junctions. Thus, breaking all curves at corners, *i.e.* high-curvature points, should remedy this problem, Figure 13. Unfortunately, it is difficult to output curvature for noisy curves, thus requiring a smoothing algorithm before the curve can be broken at high-curvature points. This smoothing algorithm is described below in the context of curve noise.

Problem 2: Lofting sensitivity to curve noise: Curve fragments of the 3D drawing can have excessive noise,

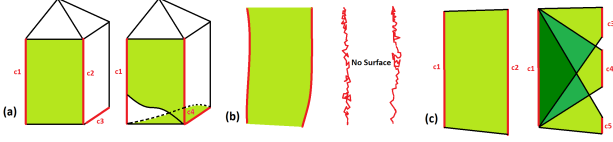


Figure 12: (a) Overgrouping of two curve fragments C_2 and C_3 into C_4 can lead to nonsensical lofting results in the pair (C_1, C_4) in contrast to the close-to-veridical results of lofting (C_1, C_2) ; (b) lofting is sensitive to loop-like noise or excessive perturbations; (c) lofting with overfragmented curves produces suboptimal lofting results and redundant surface proposals, leading to a combinatorial increase in the number of lofting applications and postprocessing.

depicting loop-like structures and local perturbations, Figure 12b. These degeneracies in the local form of a curve fragment often result in failures in the lofting algorithm to produce a surface hypothesis, or result in surfaces featuring geometric degeneracies. There are a number of smoothing methods, and we use a relatively recent robust algorithm that is based on B-splines [14, 15], balancing data fidelity term with a smoothness term. The ratio of those two terms determine the degree of smoothing. The advantage of this method is that the polyline representation of the curve can be maintained after smoothing.

Problem 3: Lofting sensitivity to overfragmentation and gaps: Lack of edges or undergrouping in the edge grouping stage can lead to gaps and overfragmentation. In both cases, a long veridical curve is represented as multiple smaller curve fragments, Figure 12c. As a result, what would have been a single surface patch now needs to be covered by a suboptimal set of smaller, overlapping surface hypotheses. In addition, the increased number of curve fragments increases the number of curve pairs to be considered, and lead to a combinatorial increase in computational cost. Curve fragments that are coincidental at a point can be grouped if they show good continuity of tangents at endpoints. Similarly, gaps between two curve fragments $\Gamma_1(s)$ and $\Gamma_2(s)$ can be bridged between endpoint $\Gamma_1(s_1)$ and $\Gamma_2(s_2)$ if: (i) These endpoints are sufficiently close, *i.e.*, $|\Gamma_1(s_1) - \Gamma_2(s_2)| < \tau_{dist}$, where τ_{dist} is a gap proximity threshold, and (ii) $CC((\Gamma_1(s_1), T_1(s_1)), (\Gamma_2(s_2), T_2(s_2))) < \tau_{cocirc}$ where CC is the co-circularity measure, characterizing good continuation from one point-tangent pair (P_1, T_1) to another pair (P_2, T_2) [40].

Problem 4: Duplications due to curve fragment overlaps: There is some duplication in 3D curve fragments in that two curves can overlap along portions, thus creating duplicate surface representations. While this duplication may not be an issue for some applications, better results can be obtained if the duplication is removed: When two curves overlap, the longer curve is unaltered and the overlapping segment is removed from the shorter curve. The curves are

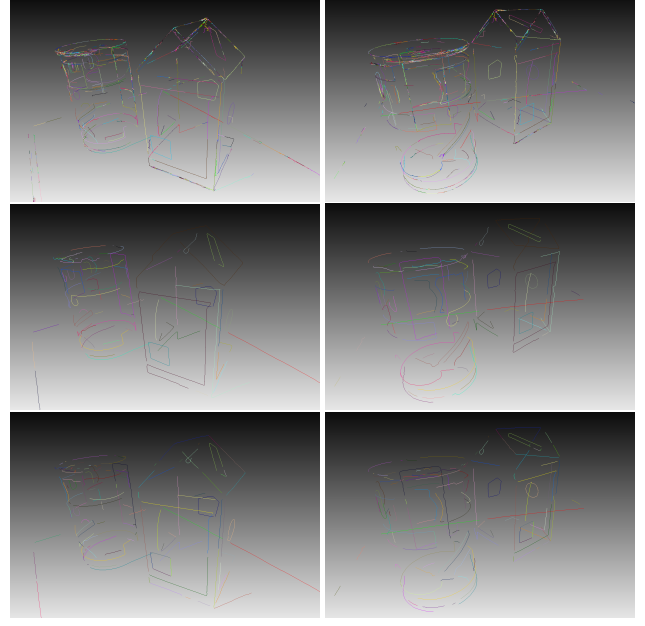


Figure 13: The original input 3d curve drawing (top row), which is the direct output of the 3D curve drawing approach, the result of our reorganization algorithm before breaking sharp corners (middle row), and after the sharp corners are broken (bottom row). The level of granularity displayed in the last row is the most appropriate for our lofting approach, as most surfaces are bounded by entire curves rather than subsegments.

also downsampled since the initial curve drawing is dense in sample points.

The resolution of the above four problems significantly improves the performance of our algorithm. Note that these steps are applied in sequence: Pruning small curves, smoothing curve fragments, gap filling and grouping overfragmented segments, eliminating duplications and downsampling. In addition, it is judicious to iteratively apply these steps in sequence, starting with small parameters and increasing the parameters in steps (typically 3-4). This is crucial because all of these steps run the risk of distorting the 3D data in significant ways if pursued too aggressively in a single iteration, *e.g.*, corners can be oversmoothed, wrong gaps can be filled, meaningful but relatively short curve fragments can get pruned without getting a chance to be merged into a larger curve fragment etc.

It should be noted that aforementioned problems do not arise in the plethora of interactive surface lofting approaches, as a human agent is available to break or group 3D structures to obtain geometrically accurate 3D surfaces, [38]. Some of the lofting approaches try to get around this problem by constraining the input curves to be closed curves, [55, 45], but a fully automated, bottom-up lofting system like ours has to be able to handle such grouping inconsistencies algorithmically.

In summary, this regrouping algorithm exploits the underlying organization, as well as the rich differential geometric properties embedded in any sufficiently-smooth, 3D curve representation, to adjust the granularity and connectivity of any input curve graph or network to suit the needs of a wide variety of applications. In the case of surface lofting, the quality of the resulting reconstructions are significantly improved if the input curves that have 3D surfaces between them have their samples more or less linearly aligned with each other, resulting in a more robust quadrangulation step that kickstarts most lofting approaches. We therefore use the 1st and 2nd order differential geometric cues, namely tangents and curvatures, to full extent in order to aggressively group smooth segments and break curves at high-curvature points, maximizing the likelihood that the lofting algorithm will receive a set of 3D curves best suited for its capabilities.

6. Experiments and Results

Implementation: The 3D drawing is computed using code made available by the authors of [51]. Smoothing code was made available by [14]. We have selected one of the most robust lofting implementations, BSurfaces, a part of Blender [11], a well-known, professional-grade CAD system in widespread use. BSurfaces is able to work on multiple curves with arbitrary topology and configurations, either simultaneously or incrementally, producing simple and smooth surfaces that accurately interpolate input curves, even if they only partially cover the boundary of the surface to be reconstructed. The use of BSurfaces has been limited to interactive modeling, where a human agent provides clean well-connected curves to the system. To the best of our knowledge, a fully-automated 3D modeling pipeline that obtains a 3D curve network, and uses lofting to surface this network in a fully-automated fashion, is novel.

Datasets: We use two datasets to quantify experimental results. First, the Amsterdam House Dataset consists of 50 fully calibrated multiview images and comprises a wide variety of object properties, including but not limited to smooth surfaces, shiny surfaces, specific close-curve geometries, text, texture, clutter and cast shadows. This dataset is used to evaluate the occlusion and visibility reasoning part of our pipeline, Section 4. Second, the Barcelona Pavilion Dataset is a realistic synthetic dataset created for validating the present approach with complete control over illumination, 3D geometry and cameras. This dataset was used with its 3D mesh ground truth to evaluate the geometric accuracy of the full pipeline.

Qualitative Evaluation: Figure 14 shows our algorithm’s reconstruction and compares it to PMVS [12]. Observe that the reconstructed surface patches are glued onto the 3D drawing so that the topological relationship among surface patches is explicitly captured and represented. A key point

to keep in mind is that the two approaches are not compared to see which is better. Rather, the intent is to show the complementary nature of the two approaches and the promise of even greater performance when appearance, the backbone of PMVS, is integrated into our approach.

Quantitative Evaluation: The algorithm is quantitatively evaluated in two ways. First, we assume the input to the algorithm, the 3D curve drawing, is correct and compare ground truth to the algorithm’s results based on a common 3D drawing. Specifically, we manually construct a surface model using the curve drawing in an interactive design and modeling context using Blender. The resulting surface model then serves as ground truth (GT) since it is the best possible expected outcome of our algorithm. Both GT and algorithm surface models are sampled and a proximity threshold is used to determine if a sample belongs to the other and vice versa. Three stages of surface reconstruction are then evaluated as a precision-recall curve, Figure 15a, namely: (i) All surface hypotheses satisfying formation constraints; (ii) surface hypotheses that survive the occlusion constraint; (iii) surface hypotheses that further satisfy the visibility constraint with duplications removed. The algorithm recovers 90% of the surfaces with nearly 100% precision. The missing surfaces are those that do not occlude any structures, and therefore cannot be validated with our approach. Clearly, the use of appearance would a long way towards recovering these missing surfaces.

Second, we also quantitatively evaluate the algorithm in an end-to-end fashion, including the 3D drawing stage. Since the ground truth surfaces are not available from Amsterdam House Dataset, we resort to using Barcelona Pavilion Dataset, which has GT surfaces. Since this dataset is large, we focus our evaluation on a specific area with two chair objects. We use the same strategy to compare the final outcome of our algorithm, Figure 15b. The results show that despite a complete disregard for appearance, geometry of the surfaces together with occlusion constraint is able to recover a significant number of surface patches accurately. The recall does not reach 100% because the ground truth floor surfaces do not occlude any curves and therefore cannot be recovered.

7. Conclusions

This paper presents a fully automated dense surface reconstruction approach using geometry of curvilinear structure evident in wide baseline calibrated views of a scene. The algorithm relies on the *3D drawing*, a graph-based representation of reconstructed 3D curve fragments which annotate meaningful structure in the scene, and on lofting to create surface patch hypotheses which are glued onto the 3D drawing, viewed as a scaffold of the scene. The algorithm validates these hypotheses by reasoning about occlusion among curves and surfaces. Thus it requires views

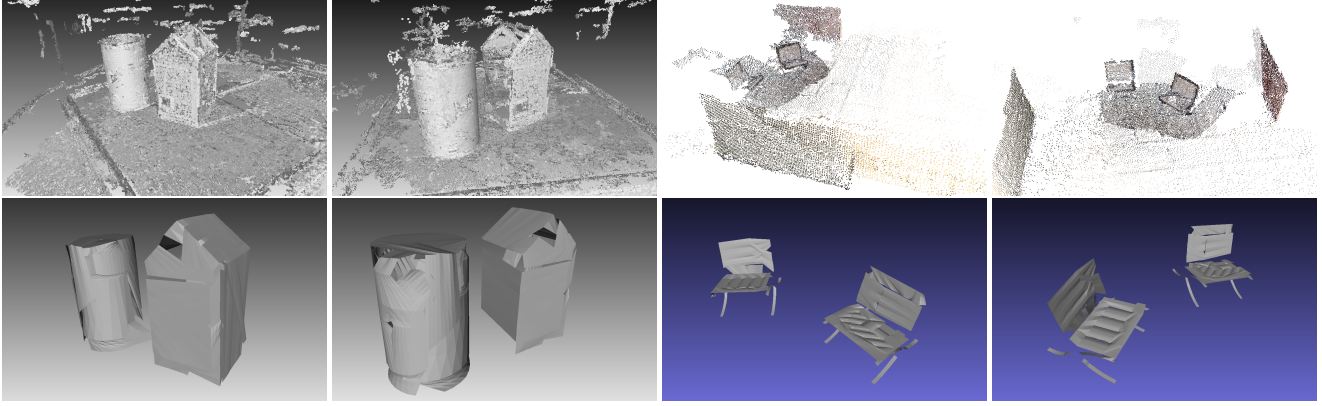


Figure 14: Two views of the PMVS reconstruction results on the Amsterdam House Dataset and Barcelona Pavilion Dataset (first row). Observe the wide gaps on homogeneous surfaces. The second row shows the results of our algorithm from the same views, obtained from a set of mere 27 curve fragments and without using appearance. Note that the PMVS gaps are filled in our results. Our algorithm errs in reconstructing the back of the can as a flat surface. This can easily be corrected via integration of appearance cues in the reconstruction process.

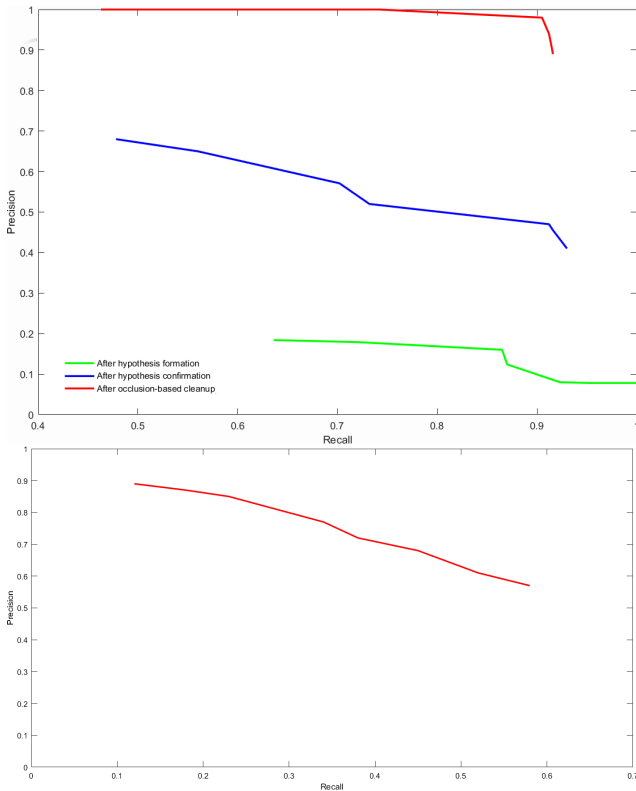


Figure 15: (a) The precision-recall curves for Amsterdam House Dataset, corresponding to post hypothesis-formation surfaces (green), confirmed surface (blue), and confirmed surfaces after occlusion-based cleanup (red). These results provide quantitative proof for the necessity of all steps in our reconstruction algorithm; (b) The precision-recall curve for Barcelona Pavilion Dataset, evaluating the geometric accuracy of the entire pipeline.

from a wide range of camera angles and performs best if there are multiple objects to afford the opportunity for inter-object and intra-object occlusion. Qualitative and quantitative evaluations shows that a significant portion of the scene surface structure can be recovered and its topological structure is made explicit, a clear advantage. This is significant considering this is only the first step in our approach, namely, using geometry without using appearance which is the core idea underlying successful dense reconstruction systems like PMVS. Our goal is to integrate the use of appearance in the process which promises to significantly improve the reconstruction performance.

References

- [1] F. Abbasinejad, P. Joshi, and N. Amenta. Surface patches from unorganized space curves. In *Proceedings of the Twenty-eighth Annual Symposium on Computational Geometry*, SoCG '12, pages 417–418, New York, NY, USA, 2012. ACM.
- [2] C. Beccari, E. Farella, A. Liverani, S. Morigi, and M. Rucci. A fast interactive reverse-engineering system. *Computer-Aided Design*, 42(10):860 – 873, 2010.
- [3] Blender Online Community. *Blender - a 3D modelling and rendering package*. Blender Foundation, Blender Institute, Amsterdam, 2016.
- [4] A. I. Bobenko and P. Schröder. Discrete willmore flow. In *Proceedings of the Third Eurographics Symposium on Geometry Processing*, SGP '05, Aire-la-Ville, Switzerland, Switzerland, 2005. Eurographics Association.
- [5] M. Bole. Revisiting traditional curve lofting to improve the hull surface design process. *Ship Technology Research*, 2015.
- [6] M. T. Bui, J. Kim, and Y. Lee. 3d-look shading from contours and hatching strokes. *Computers and Graphics*, 51:167 – 176, 2015. International Conference Shape Modeling International.

- [7] C. E. Catalano, I. Ivriissimtzis, and A. Nasri. Subdivision surfaces and applications. In L. De Floriani and M. Spagnuolo, editors, *Shape Analysis and Structuring*, pages 115–143. Springer Berlin Heidelberg, Berlin, Heidelberg, 2008.
- [8] H. Chiyokura and F. Kimura. Design of solids with free-form surfaces. *SIGGRAPH Comput. Graph.*, 17(3):289–298, July 1983.
- [9] K. Das, P. Diaz-Gutierrez, and M. Gopi. Sketching Free-form Surfaces Using Network of Curves. In J. A. P. Jorge and T. Igarashi, editors, *Eurographics Workshop on Sketch-Based Interfaces and Modeling*. The Eurographics Association, 2005.
- [10] T. DeRose, M. Kass, and T. Truong. Subdivision surfaces in character animation. In *Proceedings of the 25th Annual Conference on Computer Graphics and Interactive Techniques*, SIGGRAPH '98, pages 85–94, New York, NY, USA, 1998. ACM.
- [11] L. Eclectiel and Blender Online Community. *Blender BSurfaces – 3D modeling and retopology software*. Blender Foundation, Blender Institute, Amsterdam, 2016.
- [12] Y. Furukawa and J. Ponce. Accurate, dense, and robust multi-view stereopsis. In *2007 IEEE Computer Society Conference on Computer Vision and Pattern Recognition (CVPR 2007)*, 18-23 June 2007, Minneapolis, Minnesota, USA, 2007.
- [13] Y. Furukawa and J. Ponce. Accurate, dense, and robust multi-view stereopsis. *IEEE Trans. Pattern Anal. Mach. Intell.*, 32(8):1362–1376, Aug. 2010.
- [14] D. Garcia. Robust smoothing of gridded data in one and higher dimensions with missing values. *Computational Statistics and Data Analysis*, 54(4):1167 – 1178, 2010.
- [15] D. Garcia. A fast all-in-one method for automated post-processing of piv data. *Experiments in Fluids*, 50(5):1247–1259, 2011.
- [16] A. S. Glassner, editor. *An Introduction to Ray Tracing*. Academic Press Ltd., London, UK, UK, 1989.
- [17] C. Grimm and P. Joshi. Just drawit: A 3d sketching system. In *Proceedings of the International Symposium on Sketch-Based Interfaces and Modeling*, SBIM '12, pages 121–130, Aire-la-Ville, Switzerland, Switzerland, 2012. Eurographics Association.
- [18] Y. Guo, N. Kumar, M. Narayanan, and B. Kimia. A multi-stage approach to curve extraction. In *CVPR'14*, 2014.
- [19] H. Hoppe, T. DeRose, T. Duchamp, M. Halstead, H. Jin, J. McDonald, J. Schweitzer, and W. Stuetzle. Piecewise smooth surface reconstruction. In *Proceedings of the 21st Annual Conference on Computer Graphics and Interactive Techniques*, SIGGRAPH '94, pages 295–302, New York, NY, USA, 1994. ACM.
- [20] P. Kaklis and A. Ginnis. Sectional-curvature preserving skinning surfaces. *Computer Aided Geometric Design*, 13(7):601 – 619, 1996.
- [21] V. Kraevoy, A. Sheffer, and M. van de Panne. Modeling from contour drawings. In *Sketch Based Interfaces and Modeling*, New Orleans, Louisiana, USA, 2009. *Proceedings*, pages 37–44, 2009.
- [22] G. Lavou, F. Denis, and F. Dupont. Subdivision surface watermarking. Technical Report RR-LIRIS-2006-011, LIRIS UMR 5205 CNRS/INSA de Lyon/Universit Claude Bernard Lyon 1/Universit Lumire Lyon 2/cole Centrale de Lyon, June 2006.
- [23] A. Levin. Combined subdivision schemes for the design of surfaces satisfying boundary conditions. *Computer Aided Geometric Design*, 16(5):345 – 354, 1999.
- [24] A. Levin. Interpolating nets of curves by smooth subdivision surfaces. In *Proceedings of the 26th Annual Conference on Computer Graphics and Interactive Techniques*, SIGGRAPH '99, pages 57–64, New York, NY, USA, 1999. ACM Press/Addison-Wesley Publishing Co.
- [25] C.-Y. Lin, C.-S. Liou, and J.-Y. Lai. A surface-lofting approach for smooth-surface reconstruction from 3d measurement data. *Computers in Industry*, 34(1):73 – 85, 1997.
- [26] C. Loop. Second order smoothness over extraordinary vertices. In *Proceedings of the 2004 Eurographics/ACM SIGGRAPH Symposium on Geometry Processing*, SGP '04, pages 165–174, New York, NY, USA, 2004. ACM.
- [27] W. Ma, X. Ma, S.-K. Tso, and Z. Pan. A direct approach for subdivision surface fitting from a dense triangle mesh. *Computer-Aided Design*, 36(6):525 – 536, 2004.
- [28] T. Maekawa and K. Ko. Surface construction by fitting unorganized curves. *Graphical Models*, 64(5):316 – 332, 2002.
- [29] H. P. Moreton and C. H. Séquin. Functional optimization for fair surface design. In *Proceedings of the 19th Annual Conference on Computer Graphics and Interactive Techniques*, SIGGRAPH '92, pages 167–176, New York, NY, USA, 1992. ACM.
- [30] S. Morigi and M. Rucci. Reconstructing surfaces from sketched 3d irregular curve networks. In *Proceedings of the Eighth Eurographics Symposium on Sketch-Based Interfaces and Modeling*, SBIM '11, pages 39–46, New York, NY, USA, 2011. ACM.
- [31] S. Nam and Y. Chai. Spacesketch: Shape modeling with 3d meshes and control curves in stereoscopic environments. *Computers and Graphics*, 36(5):526 – 533, 2012. Shape Modeling International (SMI) Conference 2012.
- [32] A. Nasri. Curve interpolation in recursively generated b-spline surfaces over arbitrary topology. *Computer Aided Geometric Design*, 14(1):13 – 30, 1997.
- [33] A. Nasri, A. Abbas, and I. Hasbini. Skinning catmull-clark subdivision surfaces with incompatible cross-sectional curves. In *Proceedings of the 11th Pacific Conference on Computer Graphics and Applications*, PG '03, pages 102–, Washington, DC, USA, 2003. IEEE Computer Society.
- [34] A. H. Nasri. Recursive subdivision of polygonal complexes and its applications in computer-aided geometric design. *Computer Aided Geometric Design*, 17(7):595 – 619, 2000.
- [35] A. H. Nasri. Interpolating an unlimited number of curves meeting at extraordinary points on subdivision surfaces. *Comput. Graph. Forum*, 22(1):87–98, 2003.
- [36] A. H. Nasri and A. M. Abbas. Lofted catmull-clark subdivision surfaces. In *2002 Geometric Modeling and Processing (GMP 2002), Theory and Applications*, 10-12 July 2002, Wako, Saitama, Japan, pages 83–93, 2002.
- [37] A. H. Nasri, T. Kim, and K. Lee. Fairing recursive subdivision surfaces with curve interpolation constraints. In *2001*

- International Conference on Shape Modeling and Applications (SMI 2001)*, 7-11 May 2001, Genoa, Italy, page 49, 2001.
- [38] A. Nealen, T. Igarashi, O. Sorkine, and M. Alexa. Fiber-mesh: Designing freeform surfaces with 3d curves. In *ACM SIGGRAPH 2007 Papers*, SIGGRAPH '07, New York, NY, USA, 2007. ACM.
 - [39] H. Pan, Y. Liu, A. Sheffer, N. Vining, C.-J. Li, and W. Wang. Flow aligned surfacing of curve networks. *ACM Trans. Graph.*, 34(4):127:1–127:10, July 2015.
 - [40] P. Parent and S. W. Zucker. Trace inference, curvature consistency, and curve detection. *IEEE Trans. Pattern Anal. Mach. Intell.*, 11(8):823–839, Aug. 1989.
 - [41] H. Park, H. B. Jung, and K. Kim. A new approach for lofted b-spline surface interpolation to serial contours. *The International Journal of Advanced Manufacturing Technology*, 23(11):889–895, 2004.
 - [42] J. Peters and U. Reif. The simplest subdivision scheme for smoothing polyhedra. *ACM Trans. Graph.*, 16(4):420–431, Oct. 1997.
 - [43] L. Piegl and W. Tiller. Algorithm for approximate nurbs skinning. *Computer-Aided Design*, 28(9):699 – 706, 1996.
 - [44] B. Sadri and K. Singh. Flow-complex-based shape reconstruction from 3d curves. *ACM Trans. Graph.*, 33(2):20:1–20:15, 2014.
 - [45] S. Schaefer, J. Warren, and D. Zorin. Lofting curve networks using subdivision surfaces. In *Proceedings of the 2004 Eurographics/ACM SIGGRAPH Symposium on Geometry Processing*, SGP '04, pages 103–114, New York, NY, USA, 2004. ACM.
 - [46] O. Sorkine and D. Cohen-Or. Least-squares meshes. In *2004 International Conference on Shape Modeling and Applications (SMI 2004)*, 7-9 June 2004, Genova, Italy, pages 191–199, 2004.
 - [47] H. Suzuki, S. Takeuchi, and T. Kanai. Subdivision surface fitting to a range of points. In *Computer Graphics and Applications, 1999. Proceedings. Seventh Pacific Conference on*, pages 158–167, 322, 1999.
 - [48] S. Takeuchi, T. Kanai, H. Suzuki, K. Shimada, and F. Kimura. Subdivision surface fitting with qem-based mesh simplification and reconstruction of approximated b-spline surfaces. In *Computer Graphics and Applications, 2000. Proceedings. The Eighth Pacific Conference on*, pages 202–212, 2000.
 - [49] A. Tamrakar and B. B. Kimia. No grouping left behind: From edges to curve fragments. In *IEEE 11th International Conference on Computer Vision, ICCV 2007, Rio de Janeiro, Brazil, October 14-20, 2007*, pages 1–8, 2007.
 - [50] N. J. Tustison, D. Abendschein, and A. A. Amini. Biventricular myocardial kinematics based on tagged mri from anatomical nurbs models. In *Computer Vision and Pattern Recognition, 2004. CVPR 2004. Proceedings of the 2004 IEEE Computer Society Conference on*, volume 2, pages II–514–II–519 Vol.2, June 2004.
 - [51] A. Usumezbas, R. Fabbri, and B. B. Kimia. From multiview image curves to 3D drawings. In *Proceedings of the European Conference in Computer Vision*, 2016.
 - [52] W. Welch and A. Witkin. Free-form shape design using triangulated surfaces. In *Proceedings of the 21st Annual Conference on Computer Graphics and Interactive Techniques*, SIGGRAPH '94, pages 247–256, New York, NY, USA, 1994. ACM.
 - [53] C. D. Woodward. Skinning techniques for interactive b-spline surface interpolation. *Comput. Aided Des.*, 20(10):441–451, Oct. 1988.
 - [54] S.-C. Wu, J. F. Abel, and D. P. Greenberg. An interactive computer graphics approach to surface representation. *Commun. ACM*, 20(10):703–712, Oct. 1977.
 - [55] Y. Zhuang, M. Zou, N. Carr, and T. Ju. A general and efficient method for finding cycles in 3d curve networks. *ACM Transactions on Graphics (TOG)*, 32(6):180, 2013.
 - [56] D. Zorin. Modeling with multiresolution subdivision surfaces. In *ACM SIGGRAPH 2006 Courses*, SIGGRAPH '06, pages 30–50, New York, NY, USA, 2006. ACM.